Published in final edited form as:
J Magn Reson Imaging. 2009 June ; 29(6): 1425–1431. doi:10.1002/jmri.21794.

Measurement of Deep Gray Matter Perfusion Using a Segmented True FISP ASL Method at 3T

Elan J. Grossman, MS[1], **Ke Zhang, MS**[1], **Jing An, MD**[2], **Abram Voorhees, PhD**[3], **Matilda Inglese, MD, PhD**[1], **Yulin Ge, MD**[1], **Niels Oesingmann, PhD**[3], **Jian Xu, BS**[3], **Kelly A. Mcgorty, RT**[1], and **Qun Chen, PhD**[1]

[1] Center for Biomedical Imaging, Department of Radiology, New York University School of Medicine, New York, New York, USA

[2] Siemens Medical Solutions, Beijing, China

[3] Siemens Medical Solutions, Malvern, Pennsylvania, USA

Abstract

Purpose—To study the feasibility of using the magnetic resonance imaging (MRI) technique of segmented true fast imaging with steady state precession arterial spin labeling (true FISP ASL) for the noninvasive measurement and quantification of local perfusion in cerebral deep gray matter at 3T.

Materials and Methods—A flow-sensitive alternating inversion recovery (FAIR) ASL perfusion preparation was used in which the EPI readout was replaced with a segmented true FISP data acquisition strategy. The absolute perfusion for six selected regions of deep gray matter (left and right thalamus, putamen, and caudate) were calculated in eleven healthy human subjects (6 male, 5 female; mean age 35.5 years ± 9.9).

Results—Preliminary measurements of the average absolute perfusion values at the six selected regions of deep gray matter are in agreement with published values for mean absolute cerebral blood flow (CBF) baselines acquired from healthy volunteers using positron emission tomography (PET).

Conclusions—Segmented true FISP ASL is a practical and quantitative technique suitable to measure local tissue perfusion in cerebral deep gray matter at a high spatial resolution without the susceptibility artifacts commonly associated with EPI based methods of ASL.

Keywords

arterial spin labeling (ASL); cerebral blood flow (CBF); cerebral perfusion; deep gray matter perfusion; flow-sensitive alternating inversion recovery (FAIR); true fast imaging with steady state precession arterial spin labeling (true FISP ASL)

INTRODUCTION

The assessment of deep gray matter perfusion is of great clinical importance. It has significant value in elucidating pathophysiology and is of considerable interest as a diagnostic and therapeutic indicator (1–8). The vascular mechanisms associated with this

Address correspondence and reprint requests to: Elan J. Grossman, Center for Biomedical Imaging, Department of Radiology, New York University School of Medicine, 660 First Ave., 4th floor, Rm. 420, New York, NY 10016 USA. E-mail: ejg279@med.nyu.edu, Phone: (212) 263-3347, Fax: (212) 263-7541.

region serve the basal ganglia, thalamus, hypothalamus, subthalamus, and septal nuclei and are thought to be implicated in many dysfunctions including, for example, Parkinson's disease (1,2), multiple sclerosis (3,4), traumatic brain injury (5,6), and certain forms of hydrocephalus (7,8).

The range of techniques currently employed for the study of deep gray matter perfusion include positron emission tomography (PET) (6,8), single photon emission computed tomography (SPECT) (2,5), and bolus tracking gadolinium enhanced magnetic resonance imaging (MRI) (1,4). Each of these approaches require the use of exogenous endovascular contrast agents that preclude frequent repeat scanning in humans and therefore make it difficult to monitor longitudinal changes in perfusion. PET and SPECT are also not refined enough to clearly distinguish anatomy within deep gray matter and are very costly methods that are restricted to a small number of highly specialized centers. The only completely noninvasive method of investigating cerebral blood flow (CBF) that is proficient at resolving substructure, less costly, and widely available is the MRI technique of arterial spin labeling (ASL), which utilizes blood water as an endogenous, freely diffusible tracer (9–13). In the past several years a number of studies have been published reporting measurements of CBF with ASL in normal adult and pediatric subjects (14,15) and in adult subjects with various cerebrovascular and psychiatric disorders (16,17). To date, however, the application of ASL to the measurement of local perfusion in deep gray matter remains sparse. The explanation for this may be the lack of suitable techniques that are available since most methods of ASL use an echo planar imaging (EPI) based data acquisition strategy (11,12). Although EPI provides a relatively high signal-to-noise ratio (SNR) over short measuring times, it is prone to susceptibility artifacts and rapid dephasing caused by local magnetic field inhomogeneities in deep gray matter.

Several ASL data acquisition techniques have been developed recently that are insensitive to magnetic field inhomogeneity. These include rapid acquisition with relaxation enhancement (RARE) (18), gradient echo and spin echo (GRASE) (18), half-Fourier single-shot turbo spin-echo (HASTE) (19), fast low-angle shot (FLASH) (20), and turbo FLASH (21). Each of these approaches, however, is hampered by additional obstacles that make them unsuitable for quantitative measurement of perfusion in deep gray matter. Single-shot fast spin-echo (FSE) techniques such as RARE and HASTE exhibit blurring that occurs as a result of T2 decay during long echo train sequences (22), GRASE displays complex phase modulation errors (18), the application of FLASH using multiple small flip angle excitations can produce undesired saturation effects, and turbo FLASH yields a significantly diminished SNR (22).

The advent of fast high-performance MR gradient systems has led to the implementation of true fast imaging with steady state precession (true FISP) in standard clinical protocols and its development as another ASL data acquisition strategy (23,24). When a true FISP sequence is combined with a flow-sensitive alternating inversion recovery (FAIR) ASL preparation the resulting images are less sensitive to susceptibility artifacts than EPI and provide a similar SNR per measuring time without any of the disadvantages connected to spin echo approaches. This technique has recently been applied with success by Boss et al. (25) at 1.5 and 3T in three different axial slice positions of the brain, including a slice cranial to the corpus callosum, a slice close to the skull base, and a slice in the area of the cerebellum and the temporal lobe. Cerebral perfusion was estimated in gray and white matter regions exhibiting critically high magnetic susceptibility differences such as near brain-bone transitions in the frontal, parietal, occipital, and temporal lobes. In the present study we focus on applying true FISP ASL to overcoming magnetic inhomogeneity associated with cerebral deep gray matter. The measurement of perfusion within the diminutive anatomical substructures of this region requires an improvement in spatial

resolution over that which can be acquired with the single-shot version of true FISP ASL developed by Boss et al. We have therefore adopted a multi-shot segmented imaging approach to the sequence that provides a significant increase in spatial resolution (1 mm × 1 mm × 8 mm as compared to 4 mm × 4mm × 5 mm). We demonstrate that segmented true FISP ASL is a potentially valuable tool for acquiring completely noninvasive measurements of localized perfusion in cerebral deep gray matter at a high spatial resolution without the presence of susceptibility artifacts.

MATERIALS AND METHODS

True FISP ASL Sequence

A spin-labeling scheme depicting the application of true FISP ASL is graphically illustrated in Fig. 1. A FAIR ASL technique is used in which a true FISP steady-state sequence is substituted for an EPI method of signal acquisition. Descriptions of true FISP and FAIR have been previously detailed elsewhere (11–13,23,24). Slice-selective and slice-nonselective inversion pulses are interleaved to generate a set of labeled and control images respectively. In the labeled image the spins of tissue water contained in the spatially selective slice are inverted and in a different magnetization state from the fully relaxed inflowing arterial blood water located proximal to this region. In the control image, however, since it is acquired after a non-selective global inversion pulse that includes spins distal to the selective slice, both blood and tissue water in this region are in identical magnetization states. The labeled and the control images are subtracted to produce an ASL difference image in which the signal from the static spins cancel each other out leaving a signal difference map of arterial blood delivered to each voxel during an inversion time (TI) interval. This signal difference map provides a qualitative measure of local perfusion from which CBF can be calculated. An example demonstrating labeled, control, and difference images obtained using the current technique is shown in Fig. 2.

Experimentation and Data Analysis

A total of 11 healthy human subjects (6 male, 5 female; mean age 35.5 years ± 9.9) were scanned using a 3T Siemens Trio whole-body MR scanner (Siemens Medical Systems, Erlangen, Germany) that operated with a maximum gradient strength of 45 mT/m and a slew rate of 200 mT/m/ms along all three axes. A 12-element receiver head coil was used with body coil excitation. The study was approved by the institutional review board and all participants provided proper informed written consent prior to each experiment.

A segmented true FISP ASL sequence was performed in which acquisition was from a 6–8 mm thick oblique-axial slice that was positioned parallel to the anterior commissure-posterior commissure (AC-PC) line at the level of the basal ganglia. A centric k-space sequential ordering scheme was used with interleaving in which 3 segments were acquired at the rate of 53 lines per segment with an acquisition time of 217.3 ms per segment. This relatively short time window was chosen to maximize the difference in ASL signal intensity. The pulse sequence included a FAIR preparation in which the inversion time (TI) was 1200 ms, the duration of the radio frequency (RF) pulse was 10.24 ms, and the recovery time between subsequent labeling pulses was 3 s. To eliminate magnetic inhomogeneities due to residual contamination from static tissue a frequency offset corrected inversion (FOCI) pulse was used (26–28). The FOCI pulse had a slice thickness of 2.5 times the thickness of the imaging slice to compensate for imperfect slice profile. Other sequence parameters for the segmented true FISP steady state precession readout included a flip angle (FA) of 50 degrees, a repetition time (TR) of 3.2–4.1 ms, an echo time (TE) of 1.6–2.1 ms, an image matrix size of 192–256 × 192–256, a field of view (FOV) of 25–30 cm, and a spatial resolution of 1 mm × 1 mm × 6–8 mm. One labeled and one control image were acquired

with 8 averages. A spoiler gradient was applied during the slice selective inversion pulses that had a strength of 8 mT/m and a duration of 9 ms. One section was acquired per measurement and the total scan time for each sequence was about 2.5 minutes. In order to correct for the imperfect subtraction of stationary tissue between control and labeled images due to off-resonance effects, an approach described by Figueiredo et al. (29) was adapted in which an extra pair of images was acquired at a very short inversion time (TI_0 = 100 ms), when no perfusion effects were expected. To determine the equilibrium magnetization of tissue (M_0), another separate scan was performed using the same segmented true FISP sequence, but in the absence of an inversion-recovery preparation.

Figure 2 shows outlines of the six gray matter regions of interest (ROIs) that were selected for absolute perfusion quantification in all eleven subjects, which included the right and left thalamus, putamen, and caudate. The ROIs were first drawn manually by the same individual using the software Image J (National Institutes of Health, Bethesda, MD, USA) on a control or spin labeled image, and then copied to other corresponding images in order to obtain the matched size and location for measuring the localized signal intensities in each subject. Absolute perfusion in each of these localized areas of deep gray matter was quantified with in-house MATLAB (Mathworks, Natick, MA, USA) scripts using a general kinetic model described by Buxton et al. (30) and Yang et al. (31) as well as T_1 values obtained from published works (T_1 thalamus = 986 ms ± 33; T_1 putamen = 1102 ms ± 40; T_1 caudate = 1158 ms ± 55) (32).

To compare the image quality of true FISP with EPI additional scans were performed on one subject with both pulse sequences in which data was acquired from an 8 mm thick oblique-axial slice along the AC-PC reference line. For complete assessment a segmented approach using a 256 × 256 image matrix and a single-shot approach using 256 × 256, 128 × 128, and 64 × 64 image matrices were performed in either case. Since true FISP and EPI also employ different phase encoding strategies, right-left (RL) and anterior-posterior (AP) respectively, each EPI scan was implemented using an example of both acquisition schemes. To further maintain consistency all true FISP and EPI scans incorporated a similar spatial resolution at each matrix size (1 mm × 1 mm × 8 mm, 2 mm × 2 mm × 8 mm, and 4 mm × 4 mm × 8 mm) and a TI of 1200 ms. The true FISP scans included a bandwidth (BW) of 651 Hz/pixel, an FA of 60 degrees, a TR of 4.2 ms, and a TE of 2.1, 1.8, and 1.64 ms for the 256 × 256, 128 × 128, and 64 × 64 image matrices respectively. All other true FISP sequence parameters were identical to those described earlier. The EPI scans were standard acquisitions that included a BW of 1148 Hz/pixel and an echo spacing of 1.25 ms. For segmented EPI RL and AP scans the TEs were 69 and 63 ms respectively; for EPI single shot RL scans the TEs were 55, 24, and 15 ms for the 256 × 256, 128 × 128, and 64 × 64 image matrices respectively; and for single shot EPI AP scans the TEs were 69, 30, and 18 ms for the 256 × 256, 128 × 128, and 64 × 64 image matrices respectively.

RESULTS

Examples of labeled (slice-selective inversion) and control (slice-nonselective inversion) images obtained with segmented true FISP ASL are shown in Fig. 2a and b. The signal intensity of the labeled image is higher due to the fully relaxed, un-inverted arterial blood water that is flowing into the tissue space of the slice-selective region. A qualitative map showing relative cerebral blood flow, calculated as the difference between the labeled and control images, is displayed in Fig. 2c. Note that the signal difference is observed to be greater in gray matter than in white matter, reflective of the higher perfusion values expected in these regions.

Figure 3 compares the image quality of true FISP and EPI independent of an ASL preparation at the level of the basal ganglia. Both pulse sequences were implemented with comparable imaging parameters using segmented and single-shot approaches at different image matrix sizes with EPI having been acquired by means of both RL and AP phase encoding strategies. It can be seen from these images that segmented true FISP eliminates blurring associated with a single-shot approach that makes it difficult to identify anatomical substructures found within deep gray matter. Furthermore, while true FISP does not exhibit any indication of magnetic field distortion artifacts, EPI displays significant evidence of such effects. While the degree of distortion can be dramatically reduced in EPI by employing a segmented approach, the effect is still markedly pronounced.

Figure 4 compares the relative signal differences between segmented true FISP ASL labeled and control images obtained from one subject in the six deep gray matter regions at different TIs (100, 200, 300, 400, 500, 700, 900, 1100, 1300, 1500, 1700, 1900, 2100, 2300, 2500, and 2700 ms) with a theoretical ASL curve generated using a least squares best fit based on the model of Buxton et al. (30). These results demonstrate a good agreement between the experimental data and the standard theoretical model. The transit delay time (δt) measured in the six ROIs ranged between 0.202 s and 0.410 s with an average value of 0.313 s. Based on these data, a transit delay time of 310 ms was used for the estimation of perfusion in all subjects. The results of the current spin-labeling scheme are consistent with previous studies that have found the transit delay time in cortical gray matter can vary from 320 ms to 830 ms as the distance between the labeling plane and the image slice increases (33).

Figure 5 shows a bar graph of the average absolute perfusion values measured at the six selected ROIs in all eleven subjects with the mean and standard deviations indicated by the error bars. These results are consistent with mean absolute CBF baselines obtained from healthy volunteers using PET, in which the values are 44.7 ± 5.7 mL/100g/min in the thalamus, 42.6 ± 7.1 mL/100g/min in the putamen, and 38.5 ± 7.0 mL/100g/min in the caudate (8).

DISCUSSION

This study reports that the application of segmented true FISP ASL to cerebral deep gray matter in human subjects demonstrates a significant improvement in image quality over EPI based techniques, the advantages of which include higher spatial resolution with none of the distortion artifacts associated with EPI due to diamagnetic susceptibility effects. By assuming the general kinetic model of Buxton et al. (30) and Yang et al. (31), it may be feasible to apply this sequence to the measurement and quantification of absolute perfusion in local deep gray matter, the preliminary values of which are comparable to those acquired with PET. Segmented true FISP ASL may prove to be a useful noninvasive tool for the measurement of perfusion in deep gray matter. A number of issues, however, remain to be addressed.

The efficiency of the current segmented true FISP ASL spin-labeling scheme is limited to the acquisition of a single perfusion weighted image in approximately 2.5 minutes. This is a disadvantage when compared to a single-shot EPI method in which it is possible to obtain volume coverage within a similar duration. The restrictions imposed by segmented true FISP ASL preclude the possibility of conducting whole brain scans inside a reasonable time frame. Furthermore, there is an increased risk of introducing motion related artifacts caused by patient movement during the interval required for a single scan. Parallel imaging techniques have not been considered as a viable option to reducing the acquisition time because they would reduce the SNR, which is already low in ASL.

Another concern is that a single transit delay time was used for all the subjects, which may contribute to errors in perfusion quantification for individual cases. While measuring the transit delay time for each particular subject with additional scans is possible, the amount of time required to do this makes it unrealistic. To circumvent this problem another approach to consider may be to apply quantitative imaging of perfusion using a single subtraction (QUIPSS and QUIPSS II) (34), which provides a better estimate of perfusion since it takes into consideration the delay in the transit time of blood. We're currently in the process of implementing and evaluating a QUIPPS II based version of segmented true FISP ASL on our scanner with the intention of using this technique in future studies.

Finally, it is important to note that the current quantification model for true FISP ASL will break down in the presence of large intravascular signals. These are vessels with fast moving blood that pass through imaging voxels and increase perfusion estimates without actually providing nutritive delivery to the capillary bed. Such regions are apparent in Fig. 2c wherever saturation effects are observed. Spin labeling experiments usually employ a crusher gradient pulse in their imaging sequence to dephase signals from rapid vascular flows and eliminate them as a possible source of overestimation (13,35). A disadvantage of true FISP ASL is that at the present there is no known way to combine it with such a technique. In the current approach that has been described voxels containing large intravascular signal were scrupulously avoided during post processing. Nevertheless, small blood vessels may still provide a substantial contribution to tissue perfusion measurements through partial volume effects. It should be pointed out, however, that in a 3T magnet the signal yield may increase the spatial resolution high enough to better isolate regions of arterial flow and avoid the influence of strong partial volume effects. In high resolution studies of perfusion at 3T blood flow values measured in cortical gray matter using true FISP ASL were found to be similar to those obtained with EPI based methods of ASL in which crusher gradients were applied (25).

In conclusion, we have shown that segmented true FISP ASL is a practical and quantitative technique suitable to measure local tissue perfusion in cerebral deep gray matter at a high spatial resolution without the susceptibility artifacts commonly associated with EPI based methods of ASL. When absolute perfusion is quantified with this technique using a general kinetic model, it yields measurements that are in agreement with published values for PET. These preliminary results indicate that segmented true FISP ASL may be of value for completely noninvasive investigations of perfusion in deep gray matter.

Acknowledgments

Part of this study was supported by the National Institutes of Health (NIH) grant numbers R01HL069023-04, R01NS029029-16, R01NS039135-06A1, and R01NS051623.

References

1. Brusa L, Bassi A, Pierantozzi M, et al. Perfusion-weighted dynamic susceptibility (DSC) MRI: basal ganglia hemodynamic changes after apomorphine in Parkinson's disease. Neurol Sci. 2002; 23:S61–S62. [PubMed: 12548344]
2. Vaamonde J, Flores JM, Gallardo MJ, Ibanez. Subacute hemicorporal Parkinsonism in 5 patients with infarcts of the basal ganglia. J Neural Transm. 2007:1463–1467. [PubMed: 17705041]
3. Inglese M, Adhya S, Johnson G, et al. Perfusion magnetic resonance imaging correlates of neuropsychological impairment in multiple sclerosis. J Cereb Blood Flow Metab. 2007; 27:1–8. [PubMed: 16685255]
4. Inglese M, Park S, Johnson G, et al. Deep gray matter perfusion in multiple sclerosis. Arch Neurol. 2007; 64:196–202. [PubMed: 17296835]

5. Abu-Judeh HH, Parker R, Aleksic S, et al. SPECT brain perfusion findings in mild or moderate traumatic brain injury. Nucl Med Rev Cent East Eur. 2000; 3:5–11. [PubMed: 14600973]
6. Nakamizo A, Inamura T, Amano T, et al. Decreased thalamic metabolism without thalamic magnetic resonance imaging abnormalities following shearing injury to the substantia nigra. J Clin Neurosci. 2002; 9:685–688. [PubMed: 12604285]
7. Owler BK, Pickard JD. Normal pressure hydrocephalus and cerebral blood flow: a review. Acta Neurol Scand. 2001; 104:325–342. [PubMed: 11903086]
8. Owler BK, Momjian S, Czosnyka Z, et al. Normal pressure hydrocephalus and cerebral blood flow: a PET study of baseline values. J Cereb Blood Flow Metab. 2003; 24:17–23. [PubMed: 14688613]
9. Detre JA, Leigh JS, Williams DS, Korestky AP. Perfusion imaging. Magn Reson Med. 1992; 23:37–45. [PubMed: 1734182]
10. Edelman RR, Siewert B, Darby DG, Thangaraj V, Nobre AC, Mesulam MM, Warach S. Qualitative mapping of cerebral blood flow and functional localization with echo-planar MR imaging and signal targeting with alternating radio frequency. Radiology. 1994; 192:513–520. [PubMed: 8029425]
11. Kim SG. Quantification of relative cerebral blood flow change by flow-sensitive alternating inversion recovery (FAIR) technique; application to functional mapping. Magn Reson Med. 1995; 34:293–301. [PubMed: 7500865]
12. Kwong KK, Chesler DA, Weiskoff RM, et al. MR perfusion studies with T1- weighted echo-planar imaging. Magn Reson Med. 1995; 34:878–887. [PubMed: 8598815]
13. Calamante F, Thomas DL, Pell GS, Wiersma J, Turner R. Measuring cerebral blood flow using magnetic resonance imaging techniques. J Cereb Blood Flow Metab. 1999; 19:701–735. [PubMed: 10413026]
14. Parkes LM, Rashid WR, Chard DT, Tofts PS. Normal cerebral perfusion measurements using arterial spin labeling: reproducibility, stability, and age and gender effects. Magn Reson Med. 2004; 51:736–743. [PubMed: 15065246]
15. Biagi L, Abbruzzese A, Bianchi MC, Alsop DC, Del Guerra A, Tosetti M. Age dependence of cerebral perfusion assessed by magnetic resonance continuous arterial spin labeling. J Magn Reson Imaging. 2007; 25:696–702. [PubMed: 17279531]
16. Alsop DC, Detre JA, Grossman M. Assessment of cerebral blood flow in Alzheimer's disease by spin-labeled magnetic resonance imaging. Ann Neurol. 2000; 47:93–100. [PubMed: 10632106]
17. Chalela JA, Alsop DC, Gonzalez-Atavales JB, Maldjian JA, Kasner SE, Detre JA. Magnetic resonance perfusion imaging in acute ischemic stroke using continuous arterial spin labeling. Stroke. 2000; 31:680–687. [PubMed: 10700504]
18. Crelier GR, Hoge RD, Munger P, Pike GB. Perfusion-based functional magnetic resonance imaging with single-shot RARE and GRASE acquisitions. Magn Reson Med. 1999; 41:132–136. [PubMed: 10025620]
19. Liu HL, Kochunov P, Hou J, et al. Perfusion-weighted imaging of interictal hypoperfusion in temporal lobe epilepsy using FAIRHASTE: comparison with H(2)(15)O PET measurements. Magn Reson Med. 2001; 45:431–435. [PubMed: 11241700]
20. Tsekos NV, Zhang F, Merkle H, Nagayama M, Iadecola C, Kim SG. Quantitative measurements of cerebral blood flow in rats using the FAIR technique: correlation with previous iodoantipyrine autoradiographic studies. Magn Reson Med. 1998; 39:564–573. [PubMed: 9543418]
21. Pell GS, Lewis DP, Ordidge RJ, Branch CA. TurboFLASH FAIR imaging with optimized inversion and imaging profiles. Magn Reson Med. 2004; 51:46–54. [PubMed: 14705044]
22. Constable RT, Gore JC. The loss of small objects in variable TE imaging: implications for FSE, RARE, and EPI. Magn Reson Med. 1992; 28:9–24. [PubMed: 1435225]
23. Oppelt A, Graurann R, Barfuss H, Fischer H, Hartl W, Shajor W. FISP: a new fast imaging sequence. Electromedica. 1986; 54:15–18.
24. Martirosian P, Klose U, Mader I, Schick F. FAIR true-FISP perfusion imaging of the kidneys. Magn Reson Med. 2004; 51(2):353–361. [PubMed: 14755661]
25. Boss A, Martirosian P, Klose U, Nagele T, Claussen CD, Schick F. Fair-TrueFISP imaging of cerebral perfusion in areas of high magnetic susceptibility differences at 1.5 and 3 Tesla. J Magn Reson Imaging. 2007; 25:924–931. [PubMed: 17410577]

26. Ordidge RJ, Wylezinska M, Hugg JW, Butterworth E, Franconi F. Frequency offset corrected inversion (FOCI) pulses for use in localized spectroscopy. Magn Reson Med. 1996; 36:562–566. [PubMed: 8892208]
27. Yongbi MN, Branch CA, Helpern JA. Perfusion imaging using FOCI RF pulses. Magn Reson Med. 1998; 40:938–943. [PubMed: 9840841]
28. Yongbi MN, Yang Y, Frank JA, Duyn JH. Multislice perfusion imaging in human brain using C-FOCI inversion pulse: comparison with hyperbolic secant. Magn Reson Med. 1999; 42:1098–1105. [PubMed: 10571931]
29. Figueiredo PM, Clare S, Jezzard P. Quantitative perfusion measurements using pulsed arterial spin labeling: effects of large region-of-interest analysis. J Magn Reson Imaging. 2005; 21:676–682. [PubMed: 15906323]
30. Buxton RB, Frank LR, Wong EC, Siewert B, Warach S, Edelman RR. A general kinetic model for quantitative perfusion imaging with arterial spin labeling. Magn Reson Med. 1998; 40:383–396. [PubMed: 9727941]
31. Yang Y, Frank JA, Hou L, Ye FQ, McLaughlin AC, Duyn JH. Multislice imaging of quantitive cerebral perfusion with pulsed arterial spin labeling. Magn Reson Med. 1998; 39:825–832. [PubMed: 9581614]
32. Lu H, Nagae-Poetscher LM, Golay X, Lin D, Pomper M, van Zijl PC. Routine clinical brain MRI sequences for use at 3.0 Tesla. J Magn Reson Imaging. 2005; 22:12–22.
33. Parkes L, Tofts PS. Improved accuracy of human cerebral blood perfusion measurements using arterial spin labeling: accounting for capillary water permeability. Magn Reson Med. 2002; 48:27–41. [PubMed: 12111929]
34. Wong EC, Buxton RB, Frank LR. Quantitative imaging of perfusion using a single subtraction (QUIPSS and QUIPSS II). Magn Reson Med. 1998; 39:702–708. [PubMed: 9581600]
35. Ye FQ, Mattay VS, Jezzard P, Frank JA, Weinberger DR, McLaughlin AC. Correction for vascular artifacts in cerebral blood flow values measured by using arterial spin tagging techniques. Magn Reson Med. 1997; 37:226–235. [PubMed: 9001147]

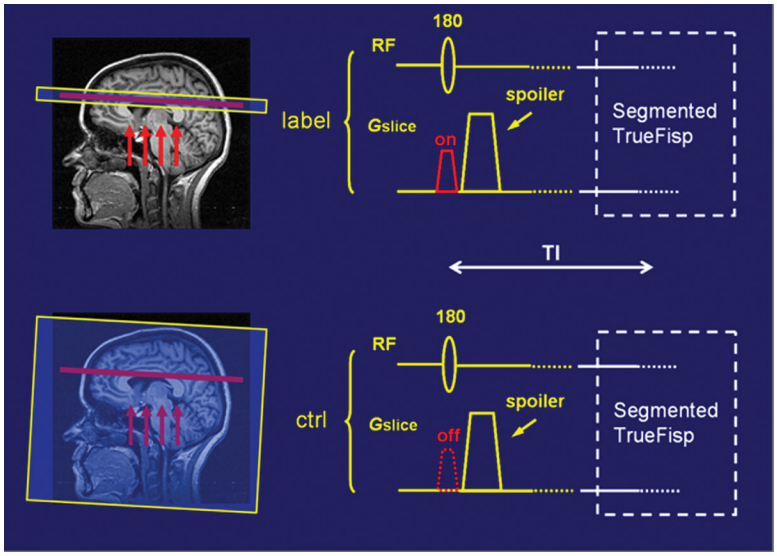

Figure 1.
A spin-labeling scheme showing how a true FISP sequence is combined with a FAIR ASL preparation in which slice-selective (top) and slice-nonselective (bottom) inversion pulses are applied alternately to generate labeled and control images respectively. The arrows indicate the direction of blood flow.

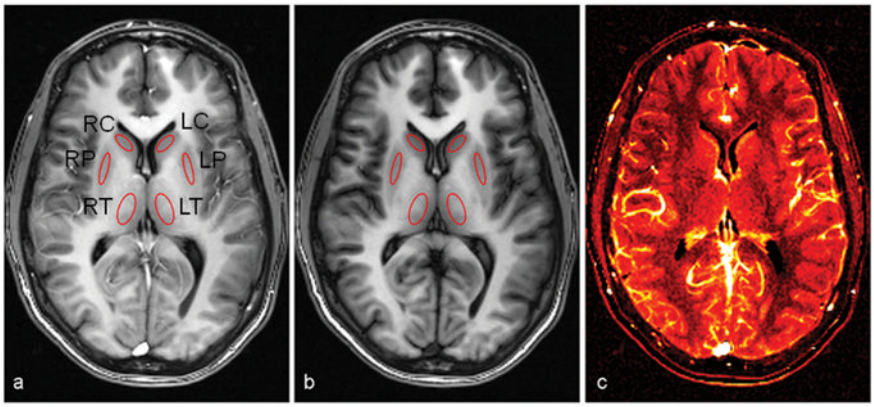

Figure 2.
A representative set of segmented true FISP ASL images acquired using eight averages. A slice-selective inversion recovery label (a) and a slice-nonselective inversion recovery control (b) are subtracted to produce a difference image (c), which provides a qualitative map in which regions with a brighter signal denote greater local perfusion. Absolute perfusion values were calculated at six deep gray matter regions indicated by the ROIs, which include the right and left thalamus (RT and LT), right and left putamen (RP and LP), and right and left caudate (RC and LC).

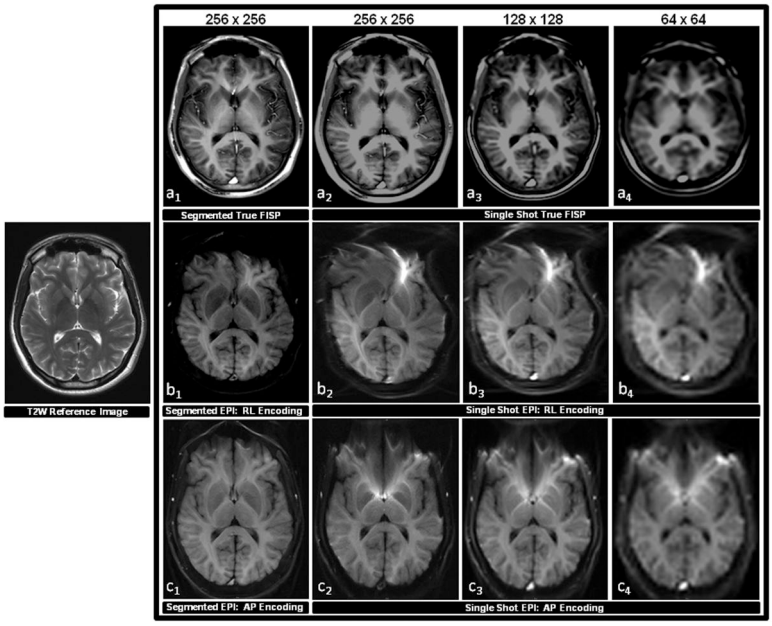

Figure 3.

A comparison of the image quality acquired with true FISP and EPI pulse sequences in the absence of an ASL preparation. Scans were obtained by applying equivalent imaging parameters to one healthy subject in the same oblique-axial slice position parallel to the AC-PC line at the level of the basal ganglia. Each pulse sequence employed a segmented approach using a 256 × 256 image matrix corresponding to an in-plane resolution of 1 mm, and a single-shot approach using 256 × 256, 128 × 128, and 64 × 64 image matrices corresponding to in-plane resolutions of 1 mm, 2 mm, and 4 mm. A T2 weighted (T2W) structural scan was also acquired at same slice position and is shown on the left for anatomical reference. The top row (a_1–a_4) shows the results of the true FISP scans, the middle row (b_1–b_4) shows the results of the EPI scans implemented with an RL phase encoding scheme, and the bottom row (c_1–c_4) shows the results of the EPI scans implemented with an AP phase encoding scheme. It can be observed from this series that segmented true FISP significantly diminishes blurring found in the single-shot approach that obscures anatomical substructures found within deep gray matter. Segmented true FISP also does not display any of the magnetic field distortion artifacts that are evident with EPI. The amount of distortion can be significantly curtailed in EPI through the application of a segmented approach, but the effect still remains distinctly evident.

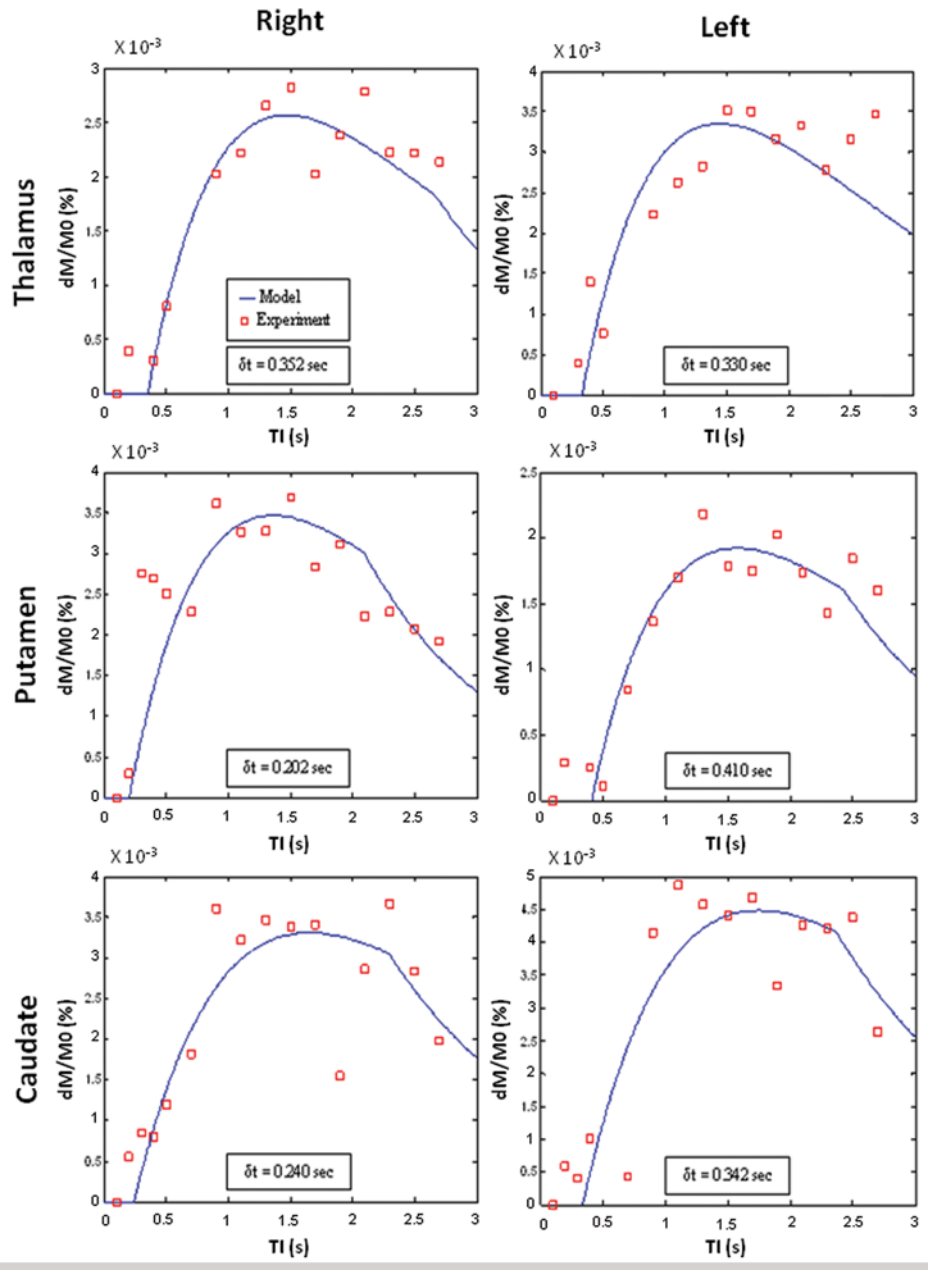

Figure 4.

Segmented true FISP ASL signal differences measured at different TIs (squares) in a healthy subject for each of the six ROIs identified in Fig. 2a and b compared to theoretical curves (lines) that were generated using a least squares best fit based on the model of Buxton et al. (30). The theoretical plot for each ROI was also used to calculate its arterial transit delay time (δt).

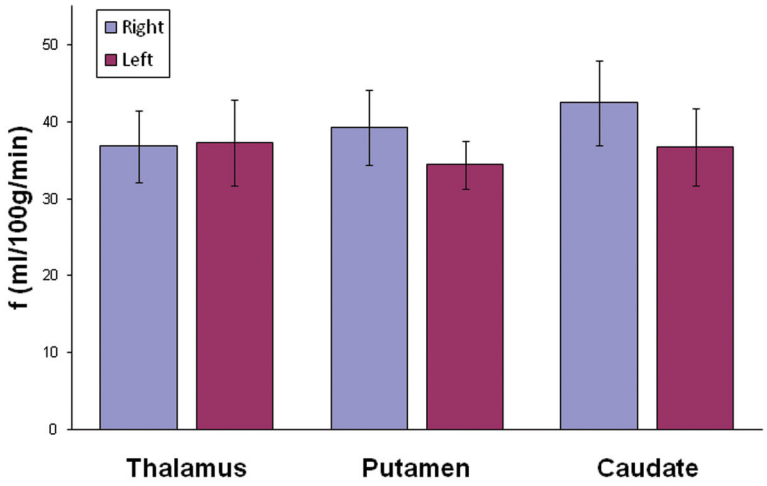

Figure 5.
The average absolute perfusion measured in the six ROIs identified in Fig. 2a and b as obtained from eleven healthy subjects using segmented true FISP ASL. The error bars represent the standard deviations.